REGULATION OF THE Na-CONDUCTING Ca CHANNEL DURING THE CARDIAC ACTION POTENTIAL

MICHELE MAZZANTI AND LOUIS J. DEFELICE
Department of Anatomy and Cell Biology, Emory University School of Medicine, Atlanta, Georgia 30322

ABSTRACT This paper describes the kinetics of an Na-conducting channel during spontaneous action potentials in beating heart cells and during simulated action potentials driven from the patch when the cell is not beating. Since the channel conducts Na only in Ca concentrations below 10^{-6} M, and since it is insensitive to tetrodotoxin and has a conductance of 100 pS in 133 mM Na, we identify it as the Ca channel conducting Na in zero Ca. By comparing the channel in beating and nonbeating cells, but under conditions in which it experiences the same voltage in both cases, we observe that: (*a*) open-channel conductance is the same in beating and nonbeating cells; (*b*) the channel reversal potential is 25 mV in beating cells and 50 mV in nonbeating cells; (*c*) the average current peaks later in beating cells than in nonbeating cells, and it has a different time course in the two cases that is not explained by the shift in reversal potential alone; and (*d*) the average Na current through Ca channels in beating cells peaks much later during the action potential than we would expect if the channel were carrying Ca. We conclude that when the Ca channel conducts Na, its kinetics and reversal potential are strongly influenced by cytoplasmic factors that accompany beating, and that its behavior is not governed by voltage alone. We also conclude that when the Ca channel conducts Na, not only are its reversal potential and conductance altered from what they would be were the channel carrying Ca, but also the channel's kinetics depend on the permeant ion. Since only the channels in the patch are in zero Ca and are conducting Na, while the Ca channels surrounding the patch are in 1.5 mM Ca and are conducting Ca, our data support the idea that it is only the Ca passing through individual channels that influences the kinetics of those same channels.

INTRODUCTION

The dynamic state of beating heart cells may be involved in the regulation of ion channel gating beyond its direct effect on membrane voltage. For example, Ca ions passing through Ca channels could be the principal source of the channel's inactivation (Mentrard et al., 1984). Lux and Brown (1984), however, in a single channel study that compares open and closed time kinetics, give evidence contrary to this hypothesis. We address the issue of channel regulation by comparing the activity of channels in beating and nonbeating heart cells and by arranging the experimental conditions so that the channel experiences the same voltage in both cases.

The low conductance of Ca channels discourages any attempt to study the current as a composition of single-channel events. For this reason, most single-channel studies use high concentrations of Ca (or other permeant divalent cations, such as Ba or Sr) to increase the single-channel conductance (see, e.g., Reuter et al., 1982). Even in 110–150 mm $[Ca]_o$, however, the conductance of the Ca channel is only 9 pS (Hess et al., 1985). The highest Ca channel conductances occur in the absence of external Ca, a condition in which the channels allow monovalent cations such as Na or Li to pass through them (Kostyuk and Krishtal, 1977*a*,*b*; Fukushima and Hagiwara, 1985; Cavalie et al., 1983; Hess et al., 1986; Levi and DeFelice, 1986). In 130–200 mM $[Na]_o$, Ca channels conducting Na have a conductance of nearly 100 pS (Hess et al., 1986; Levi and DeFelice, 1986).

To begin our study of the Ca channels in beating and nonbeating cells, we used a solution in the patch pipette that contains 133 mM Na and $<10^{-7}$ M Ca. The present experiments also used 7-d embryonic chick ventricle cells, about half of which beat spontaneously. Because of the presence of two populations of cells, this preparation allowed the comparison of single-channel events during the normal action potential (cf., Fischmeister et al., 1984) with single-channel events in nonbeating cells during simulated action potentials. Measurements during spontaneous beating involves the natural activity of the cardiac cell, such as the movement of ions through the surface membrane and the transient changes of Ca in the cytoplasm. The results of our comparison show a clear difference between the behavior of the Na-conducting Ca channel under voltage control alone and regulation of the channel in a beating cell that experiences both voltage and whatever other changes accompany beating. A preliminary report of this work appears in Mazzanti and DeFelice (1986).

METHODS

We prepared the embryonic ventricle cells by enzymatic digestion of 7-d chick embryo hearts following the procedure of DeHaan (1967). After

12–24 h in tissue culture medium and immediately before performing the experiments, we washed the cells with physiological solution at room temperature.

The composition of the bath solution is (in millimolars): 130 Na, 2 or 3.5 K, 1.5 Ca, 0.5 Mg, 2 H_2PO_4, 1 SO_4, 133.5 Cl, 5 dextrose, 10 HEPES, pH 7.35. The patch electrode contains a "zero-Ca solution" of 133 NaCl, 5 EGTA, pH 7.3: the calculated concentration of Ca in the pipette is 3×10^{-10} M. In some experiments the electrode also contains 5×10^{-6} M tetrodotoxin (TTX). In the whole-cell configuration, the electrode solution consists of 120 K, 0.1 Ca, 2 Mg, 122.1 Cl, 1.1 EGTA, 10 HEPES, pH 7.4.

We made the patch electrodes from borosilicate glass (7052; Corning Glass Works, Corning, NY) using a two-stage, modified puller (model 700C; David Kopf Instruments, Tujunga, CA). We coated the electrodes with Sylgard (Dow Corning, Midland, MI) and then fire polished them to a tip diameter of 1–3 μm, which, filled with solution, gave a resistance of 4–10 MΩ.

We used a List EPC5 amplifier to measure the voltage and a List EPC7 amplifier to measure the single-channel current. A custom-made stimulator, which generated voltage waves of different shapes and amplitudes in 1,014, 0.5-ms steps, simulated the action potential in the patch. A VCR (Panasonic Co., Secaucus, NJ) recorded the signals, which we analyzed on a digital oscilloscope (model 4094; Nicolet Instrument Corp., Madison, WI) and an IBM-AT microcomputer (IBM Instruments, Inc., Danbury, CT).

RESULTS

Two-electrode experiments allow simultaneous records of voltage and current while the cell is beating. The electrode in the whole-cell mode senses the voltage, while the electrode in the cell-attached mode measures the current, permitting immediate correlation between the action current and the action potential. With zero Ca in the current-recording pipette, Na flows inward during the repolarization phase of the action potential (Fig. 1). Na ions enter Ca channels only in the patch; the rest of the cell conducts normally (cf., Fischmeister et al., 1984; Levi and DeFelice, 1986).

By forming a patch on a nonbeating cell and then clamping the pipette solution to simulate an action potential, we examined the behavior of the channel under voltage control only. By repeating the experiment on a beating cell, but now holding the pipette at the bath potential, we observed the behavior of the channel under voltage control plus any other factors that accompany beating. Since the cells came from the 7-d ventricle, which is a midway period during development, each cell is in an unstable condition between the beating and the nonbeating state. (As an example of this imbalance, a nonbeating cell may start to beat after touching it with the patch pipette.) Fig. 2 illustrates the two experimental situations: the beating cell on the top, in which the cell drives the patch, and the nonbeating cell on the bottom, in which we drove the patch externally.

Fig. 3 compares results from the cell-driven and the patch-driven configurations: *A* depicts a two-electrode experiment on a beating cell recording an action potential and an action current simultaneously; the starting point for the action potential is in this particular case −85 mV; *C* presents a single-electrode experiment on a nonbeating cell, showing the action potential protocol that drove the patch and stimulated the action current. The starting point for the simulated action potential was the resting potential for the nonbeating cell, in this case −87 mV. (We show the simulated action potential upright in Fig. 3 for easier comparison with the spontaneous action potential. The actual stimulation was as appears in Fig. 2.)

When the channel opened at analogous positions during the action potentials, the patch-driven current was larger than the cell-driven current. *B* and *D* of Fig. 3 compare instantaneous $i(V)$ plots summarizing this difference. The extensive flickering of the channel made it nearly impossible to recognize the open state. The straight lines in Fig. 3 represent estimates of the maximum current envelope for the $i(V)$ plots. The slope of both of the lines in Fig. 3 is 100 pS, but the reversal potential is shifted from 25 mV for the

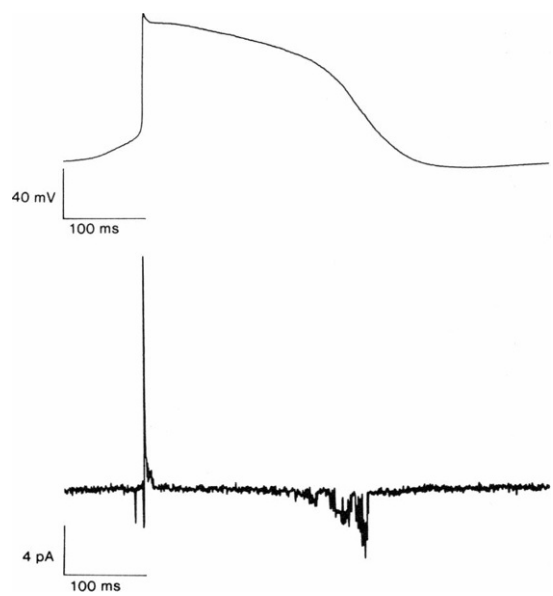

FIGURE 1 Two-electrode experiment on a beating cell. The top trace is the action potential (AP) (initial potential, −85 mV); the bottom trace is the simultaneous action current (AC). The patch-pipette contains 133 NaCl, 5 EGTA, and 5×10^{-6} M TTX. The patch contains one Na-conducting channel conducting Na inward.

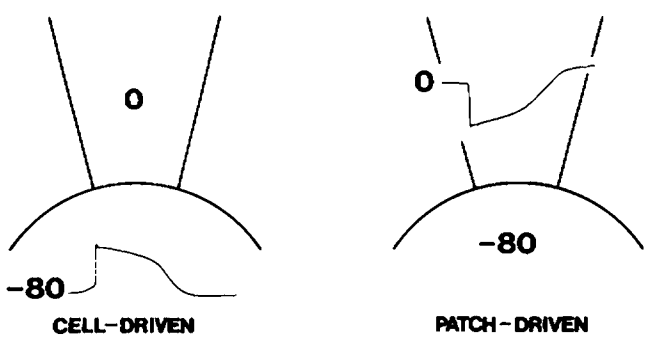

FIGURE 2 Illustration of the two categories of experiment: beating cells (cell-driven) and nonbeating cells (patch-driven). The numbers indicate millivolts.

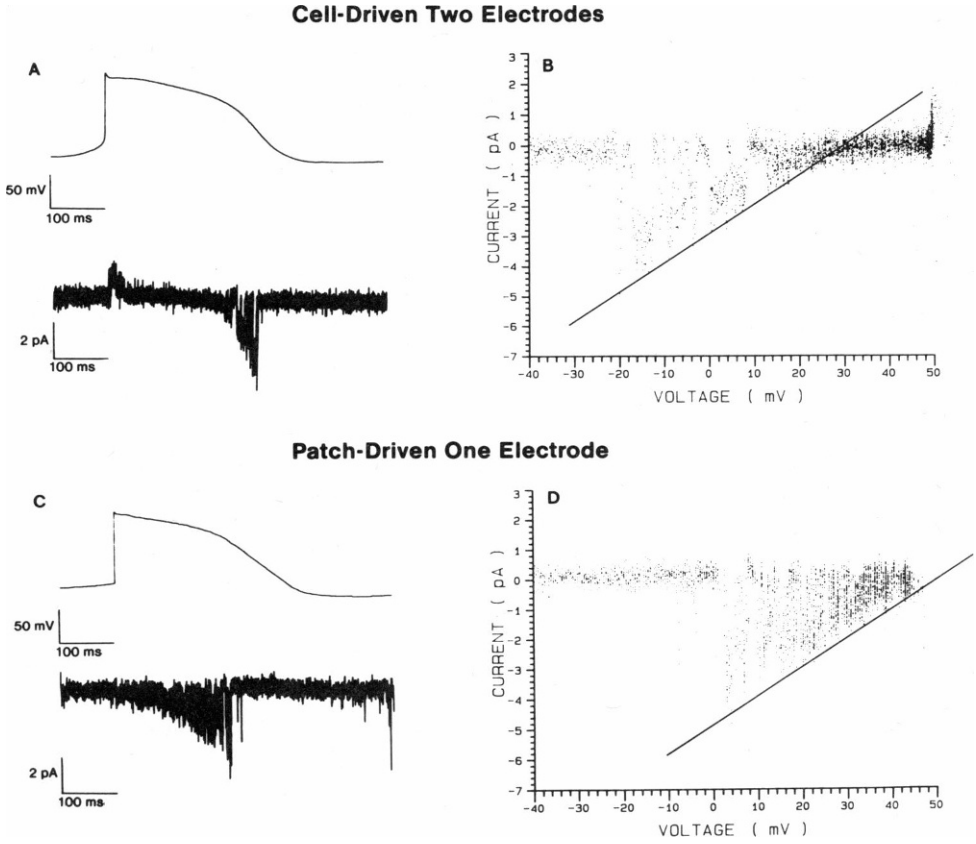

FIGURE 3 Comparison of cell-driven (two electrodes) and patch-driven (one electrode) experiments. (*A*) Cell-driven experiment; same as Fig. 1, except for subtraction of a blank trace. (*B*) Instantaneous $i(V)$ plot for the experiment in *A*. (*C*) Patch-driven experiment; the voltage protocol clamping the pipette potential generates the AC below it (after a subtraction of a blank trace). Resting potential, −87 mV. (*D*) Instantaneous $i(V)$ plot for the experiment in *C*.

cell-driven experiment to 50 mV for the patch-driven experiment.

The possibility existed that some inherent difference in Na-conducting Ca channels in beating and nonbeating cells accounted for their dissimilar response to the same voltage. Patching a cell with a slow rate of beat, and then driving the pipette with a simulated action potential between beats, resulted in a cell-driven and a patch-driven response from the same channel. Fig. 4 illustrates a patch-driven action current occurring just before a spontaneous action current. We obtained a similar pattern when the patch-driven and cell-driven action potentials were up to 30 s apart. The qualitative effect shown in Fig. 4 supports the analysis in Fig. 3, thus eliminating an inherent difference in Na-conducting Ca channels in beating and nonbeating cells as the cause of their different behavior in the two cases.

The two-electrode experiments have the disadvantage that the solution in the voltage electrode diffuses into the cell, altering physiological conditions. A single, cell-attached electrode does not have this drawback, but it introduces the problem of knowing the action potential of the beating cell. However, by selecting action currents without apparent channel activity, we were able to measure the membrane potential without breaking the patch. If traces without channels represent simple capacitive currents, then

$$i(t) = c(\mathrm{d}V/\mathrm{d}t) \tag{1}$$

or

$$\mathrm{d}V = (1/c)i(t)\mathrm{d}t. \tag{2}$$

In these equations, c is the patch capacitance, $V(t)$ is the action potential, and $i(t)$ is the action current. The integral

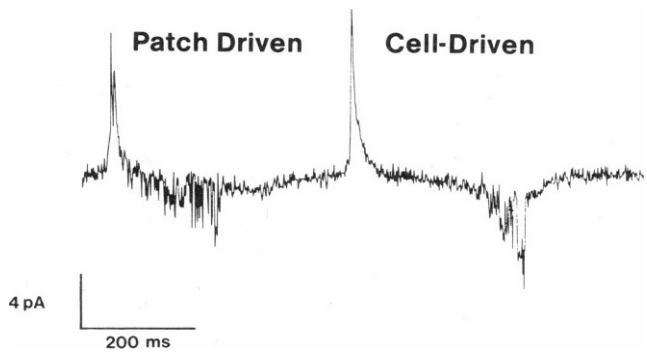

FIGURE 4 Patch-driven and cell-driven experiment on a slowly beating cell.

of a blank action current is thus proportional to the action potential.

To test whether action currents were reliable measures of the action potential, we did the experiment illustrated in Fig. 5, which compares a two-electrode experiment, measuring the action potential directly, with a one-electrode experiment in which the action potential results from integration. Fig. 5 *A* depicts simultaneous records from the same cell. Fig. 5 *B* shows a single record plus the result of its integration; the integral is in units of 10^{-15} C and represents the charge the action potential delivers to the patch. To obtain the potential from the charge requires that we know both the patch capacitance and the reference voltage. We equated the height of the charging curve to a standard action potential to measure the patch capacitance. To check whether the patch in beating and nonbeating cells experienced the same absolute potential, we broke the patch at the end of one-electrode experiments to obtain a reference voltage for each cell.

The calculated shape in Fig. 5 *B* agrees reasonably well with the measured action potential in Fig. 5 *A* except during the plateau phase. To account for this discrepancy, we assumed the blank action current contains a leak conductance (g) with zero reversal potential; in this case

$$i(t) = c(\mathrm{d}V/\mathrm{d}t) + gV(t) \tag{3}$$

or

$$\mathrm{d}V = (1/c)[i(t) - gV(t)]\mathrm{d}t. \tag{4}$$

We assumed that $V(t)$ on the right-hand side of Eq. 4 is equal to a standard action potential. By trial and error, a value of g emerged such that the integral of the square brackets in Eq. 4 was in close agreement with the recorded action potential. This value of g represents the nonspecific leak through a particular patch.

Fig. 6 includes the leak correction and compares experiments on beating and nonbeating cells using only one electrode, thus eliminating possible artifacts and possible causes of differences in channel behavior due to perfusion. The action potential-like wave in Fig. 6 *A* is the integral of the square brackets in Eq. 4 with $g = 0.5$ pS. The corrected charging curve in Fig. 6 *A* agrees more nearly with an action potential than the uncorrected curve in Fig. 5 *B*. The absolute voltage scales for the $I(V)$ plots result from matching the amplitude of the charging curve with a standard action potential and breaking the patches at the end of the experiments to obtain absolute reference potentials. The lower traces in Fig. 6, *A* and *C*, are an average of 25 action currents, each containing channel activity. The $I(V)$ relationships in Fig. 6, *B* and *D* plot these average currents against their respective action potentials.

DISCUSSION

Using 7-d ventricle cells allowed us to study Ca channels in both the beating and nonbeating state of the cell because this tissue is in a transition point during its development. In a beating cell, the channel in the patch experiences voltage plus other factors that accompany beating, such as ion fluxes through the surrounding cell membrane and the increase of intracellular Ca during contraction. In a nonbeating cell, the channel in the patch experiences only voltage plus the local flux of ions through the patch.

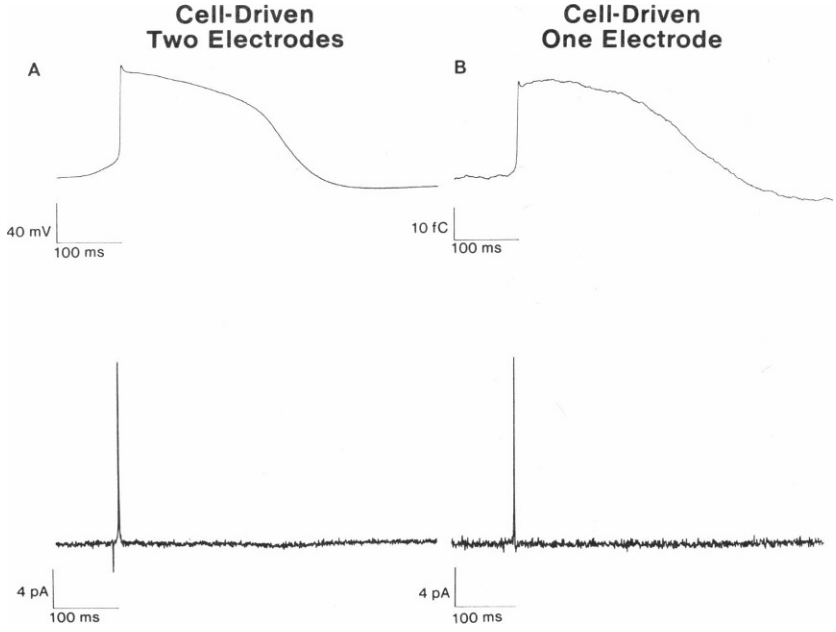

FIGURE 5 Comparison of APs and ACs from two-electrode and one-electrode experiments. (*A*) Two-electrode experiment during spontaneous activity; AP (*top*), and blank AC (*bottom*). (*B*) One-electrode experiment during spontaneous activity; the AP-like wave form (*top*) is the integral of the spontaneous AC (*bottom*).

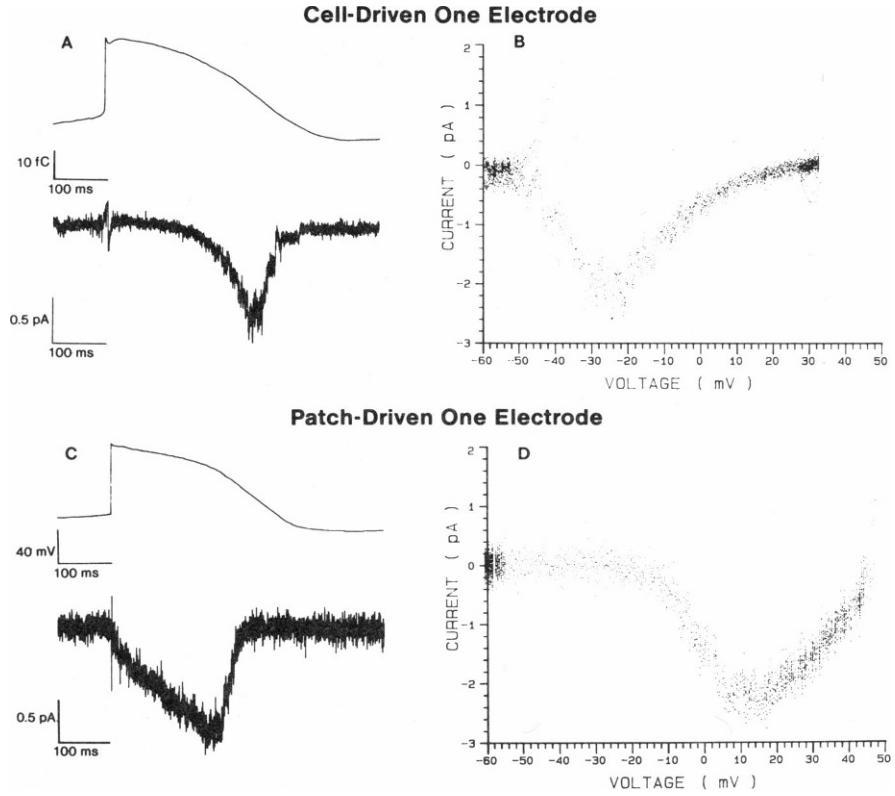

FIGURE 6 Comparison of cell-driven (one-electrode) and patch-driven (one-electrode) experiments: (*A*) Cell-driven: the AP-like wave form is the integral of an average of 40 blank ACs (corrected for leak, see Eq. 4). The current is an average of 25 ACs (with channels) minus the average of 10 blank traces. Same experiment as Fig. 5 *B*. (*B*) $I(V)$ plots for the experiment in *A*. (*C*) Patch-driven: voltage protocol (*top*); average of 25 ACs with channels (*below*), after subtraction of an average of 10 blank traces. Resting potential, −88 mV. (*D*) $I(V)$ plots for the experiments in *C*.

Although we need the action potentials and resting potentials to do the analysis, whole-cell recordings are undesirable because perfusion of the pipette's solution into the cell may influence the results. Therefore, in the final experiments comparing beating and nonbeating cells, we inferred action potentials from capacitive transients through intact patches. This procedure involved only one electrode and was, therefore, also simpler to perform.

To obtain accurate action potential shapes from current transients, it was necessary to include a leak current, $gV(t)$, in the patch. We assumed a standard form for $V(t)$ and subtracted $gV(t)$ from $i(t)$, adjusting g until a satisfactory shape emerged. The values of g satisfying this test were usually near 0.5 pS, which is the leak conductance appearing in Fig. 6. Measurements of the leakage conductance obtained by other means are generally >0.5 pS (Fischmeister et al., 1986).

From Fig. 5, an excursion of 112 mV corresponds to a charge of 17 fC, implying $c = 0.15$ pF. We could usually obtain more accurate estimates by dividing $i(t)$ by dV/dt; for example, in a patch containing no channels and low leakage, an average value over one cycle gave a patch capacitance of $c = 0.067$ pF. Alternative methods give a similar patch capacitance for electrodes of our size (Sakmann and Neher, 1983, p. 49).

The final step in deriving action potentials from cell-attached, blank action currents was to break the patch at the end of the experiment to obtain a reference potential for each cell. Possible artifacts arising from breaking the patch are the tip potential that occurs between the pipette solution and the intracellular solution and the perfusion of the cell with pipette solution that inevitably results. Comparing the potential from whole-cell recordings (using an intracellular-like solution) with the initial potential from a ruptured patch facing the test solutions showed that the tip potential was negligible in our experiments. Because of perfusion, however, only the measurements during the first few seconds after rupturing the patch were valid.

The extensive flickering of the open-channel current defeats conventional methods of defining conductance. Hess et al. (1986) found it impossible to measure Na conductance in Ca channels at ordinary pH; pH 9 reduces flickering and made the measurement feasible, suggesting to Hess et al. that protons block the open channel. In this paper we defined the conductance in the presence of flickering as the maximum envelope of the open-channel $i(V)$ scatter diagrams (Fig. 3). By this method, Ca channels conduct Na ions at a maximum conductance of 100 pS. By an alternative procedure, averaging the current during the open state, Levi and DeFelice (1986) arrived at

a lower conductance. The two methods of defining conductance resulted in the same value of this parameter for both beating and nonbeating cells.

The opposite was true for the reversal potential, which had a value of 25 mV in beating cells but 50 mV in nonbeating cells. The simplest explanation for the difference in reversal potentials is a change in internal Na concentration in beating vs. nonbeating cells. $E_{Na} = 50$ mV implies $[Na]_i = 18$ mM. Ion-selective electrodes give an internal Na value of 13 mM (Fozzard and Sheu, 1980), and flame photometry gives 30 mM (McDonald and DeHaan, 1973). To decrease E_{Na} from 50 mV in nonbeating cells to 25 mV in beating cells, $[Na]_i$ must rise from 18 to 50 mM during beating. A global increase of internal Na by 32 mM seems an unreasonably large value, but a local increase near the mouths of channels could perhaps explain the lower reversal potential in beating cells. An alternative explanation would be a decrease in Na selectivity in nonbeating cells, but at present we have no data to distinguish these two possibilities.

One difficulty in studying Na-conducting Ca channels was their disappearance and reappearance during an experiment. Although the channels were generally present in patches facing Na and EGTA, they rarely appeared to be in a steady state. This situation did not affect our studies of conductance and reversal potential, which rely only upon open-channel current, but it made the characterization of channel kinetics nearly impossible. For this reason, we decided that the absolute value of the dynamic probability of channel opening during an action potential was an unreliable parameter. However, we could obtain the maximum value of the dynamic probability by ignoring blank action currents. This selection increases the amplitude of the ensemble average but does not change its shape.

Fig. 6 results from such a selection: the ensemble averages in *A* and *C* represent the maximum $I(t)$ curves from a single channel during an action potential; *B* and *D* represent the maximum $I(V)$ curves. Both $I(t)$ and $I(V)$ have the correct shape, but their amplitudes are larger than they would be if the average had included blank action currents.

Fig. 6 shows that $I(t)$ peaks earlier in nonbeating cells, and that it has a different shape than it does in beating cells. To examine the question of whether the larger reversal potential in patch-driven channels could explain this difference, let

$$I(t) = \mathrm{Ni}(t)p(t) \tag{5}$$

and

$$i(t) = \gamma[V(t) - E] \tag{6}$$

where γ is the channel's conductance and E is its reversal potential. If Eqs. 5 and 6 are correct, E could only bias $I(t)$ vertically and could not affect its time course. The disparity between *A* and *C* in Fig. 6 implies, therefore, that $p(t)$ also depends on factors other than voltage.

The $I(V)$ curves in Fig. 6, *B* and *D*, lead to the same conclusion. Were E the only difference in the two cases, the bottom curve would be an undistorted, horizontal shift of the top curve, 25 mV to the left. Not only is the actual shift closer to 35 mV, but the shapes of the two curves are different.

For beating cells, the current peaks later during the action potential (Fig. 6 *A*) than present models for Ca channels would suggest. Since the channel is conducting Na, its reversal potential is less than it would be if the channel were conducting Ca. However, the larger Ca reversal potential would not shift the peak in Fig. 6 *A* but would only bias the curve vertically. Similarly, the lower γ of Ca vs. Na channels would only scale the curve vertically. Thus, different values of E and γ for the channel when it is conducting Ca cannot account for the late peak in current when it is conducting Na. Another explanation of the late peak in the Na current through Ca channels could be that Ca inactivates the channel it traverses, which agrees with Mentrard et al. (1984) but contradicts at least one conclusion of Lux and Brown (1984). We suggest that under the abnormal conditions of the present experiments, the channel stays open longer because Ca no longer moves through the channel. If this explanation is correct, it also implies that neither Ca from channels outside the patch, nor Ca from internal stores, can inactivate channels inside the patch, because these two sources of Ca are still intact in our experiments. This implication of our work supports one conclusion of Lux and Brown, namely that Ca ions entering the cell body do not influence Ca channels in a cell-attached patch.

In conclusion, this paper shows that when a cell beats, factors other than voltage markedly affect Na-conducting Ca channels by lowering the Na reversal potential and by retarding the peak current during the action potential. The work also suggests that Na conduction through Ca channels does not preserve normal Ca channel kinetics.

We wish to thank Ms. B. J. Duke for technical assistance in providing the tissue cultures and Mr. W. N. Goolsby for his help with electronics and computer analysis. We are grateful to Dr. Sally Wolff for editing the manuscript.

National Institutes of Health grant HL-27385 supports this work.

Received for publication 25 March 1986 and in final form 2 July 1986.

REFERENCES

Cavalie, A., R. Ochi, D. Peizer, and W. Trautwein. 1983. Elementary currents through Ca^{2+} channels in guinea pig myocytes. *Pfluegers Arch. Eur. J. Physiol.* 398:284–297.

DeHaan, R. L. 1967. Regulation of spontaneous activity and growth of embryonic chick heart cells in culture. *Dev. Biol.* 16:216–249.

Fischmeister, R., L. J. DeFelice, R. K. Ayer, Jr., R. Levi, and R. L. DeHaan. 1984. Channel currents during spontaneous action potentials in embryonic chick heart cells. The action potential clamp. *Biophys. J.* 46:267–272.

Fischmeisert, R., R. K. Ayer, and R. L. DeHaan. 1986. Some limitations of the cell-attached patch-clamp technique: a two-electrode analysis. *Pfluegers Arch. Eur. J. Physiol.* 406:73–82.

Fozzard, H. A., and S. S. Sheu. 1980. Intracellular potassium and sodium activities of chick ventricular muscle during embryonic development. *J. Physiol. (Lond.)*. 306:579–586.

Fukushima, Y., and S. Hagiwara. 1985. Currents carried by monovalent cations through Ca channels in mouse neoplastic B lymphocytes. *J. Physiol. (Lond.)*. 357:255–284.

Hess, P., and R. W. Tsien. 1984. Mechanism of ion penetration through calcium channels. *Nature (Lond.)*. 309:453–456.

Hess, P., J. B. Lansman, and R. W. Tsien. 1986. Ca channel selectivity for divalent and monovalent cations. *J. Gen. Physiol.* 88:293–319.

Kostyuk, P. G., and O. A. Krishtal. 1977*a*. Separation of sodium and calcium currents in the somatic membrane of mollusc neurones. *J. Physiol. (Lond.)*. 270:545–568.

Kostyuk, P. G., and O. A. Krishtal. 1977*b*. Effects of calcium and calcium-chelating agents on the inward and outward current in the membrane of mollusc neurones. *J. Physiol. (Lond.)*. 270:569–580.

Levi, R., and L. J. DeFelice. 1986. Sodium-conducting channels in cardiac membranes in low calcium. *Biophys. J.* 50:11–19.

Lux, H. D., and A. M. Brown. 1984. Single channel studies on inactivation of Ca currents. *Science (Wash. DC)*. 225:432–434.

Mazzanti, M., and L. J. DeFelice. 1986. Regulation of Ca channels conducting Na in the absence of external calcium involves factors other than voltage. *Biophys J.* 49(2, Pt. 2):173*a*. (Abstr.)

MacDonald, T. F., and R. L. DeHaan. 1973. Low levels and membrane potential in chick heart tissue and cultured cells. *J. Gen. Physiol.* 61:89–109.

Mentrard, D., G. Vassort, and R. Fischmeister. 1984. Calcium-mediated inactivation of the conductance in cesium loaded frog heart cells. *J. Gen. Physiol.* 83:105–131.

Reuter, H., C. Stevens, R. Tsien, and G. Yellen. 1982. Properties of single calcium channels in cardiac cell culture. *Nature (Lond.)*. 297:501–504.

Sakmann, B., and E. Neher. 1983. Geometric parameters of pipettes and membrane patches. *In* Single Channel Recording. B. Sakmann and E. Neher, editors. Plenum Publishing Corp., New York. 37–51.